Ultrafast Intramolecular Electronic Energy-Transfer Dynamics in a Bichromophoric Molecule†

Jahur A. Mondal,‡ G. Ramakrishna,‡ Ajay K. Singh,‡ Hirendra N. Ghosh,‡ M. Mariappan,§ Bhaskar G. Maiya,§ Tulsi Mukherjee,‡ and Dipak K. Palit*,‡

Radiation Chemistry & Chemical Dynamics Division, Bhabha Atomic Research Centre, Mumbai 400 085, India, and School of Chemistry, University of Hyderabad, Hyderabad 560 046, India

Received: February 16, 2004; In Final Form: March 17, 2004

Intramolecular electronic energy-transfer (intra-EET) dynamics has been investigated in 2-(9-anthryl)-1H-imidazo [4,5-f] [1,10]-phenanthroline (AIP), a newly synthesized bichromophoric molecule, using the steady-state and time-resolved absorption and fluorescence spectroscopic techniques. In AIP, anthracene (AN) and 1H-imidazo [4,5-f] [1,10]-phenanthroline (IP) molecules are directly linked to each other through a C−C σ bond and without any intervening molecular bridge. Two constituent chromophoric moieties of this bichromophoric molecule interact relatively weakly in the ground state. In the excited singlet state, however, the AN moiety transfers its excitation energy quantitatively (the efficiency of energy transfer, ϕ_{EET}, is near unity) and rapidly (the rate of energy transfer, k_{EET}, is 1.8×10^{11} s^{-1} in methanol) to the unexcited IP moiety. k_{EET} decreases linearly with increase in viscosity of the solvents, and the process is significantly retarded in rigid glass matrixes. These observations suggest that, for an efficient EET process, the molecule needs to attain a conformational geometry, which is different from that of the ground state, by undergoing a conformational relaxation process following photoexcitation. The theoretically calculated energy-transfer rate (5.1×10^9 s^{-1}) due to the Förster dipole−dipole-induced resonance-interaction mechanism is about 2 orders of magnitude smaller than the experimentally determined energy-transfer rate. Hence, the Dexter through-space exchange-interaction mechanism, which becomes predominant at shorter interchromophoric separation ($R \sim 6.3$ Å in AIP) and requires specific conformation for efficient orbital overlap, should have the major contribution to the intra-EET process in AIP. Viscosity dependence of k_{EET} suggests that we possibly measure the rate of the conformational relaxation process using the intra-EET process as the probe.

1. Introduction

Recently, a detailed understanding of the intramolecular relaxation processes in the bichromophoric molecules has attracted a great deal of interest due to the promising applications of these molecular species in molecular electronics, optical computing, artificial energy harvesting, and many other applications in photonics.[1−5] Understanding of electronic communication between the two chromophores in complex molecular systems is the key for the design and construction of efficient photonic devices. Such communication is based on the interchromophoric electronic coupling, which mediates electron and/or energy transfer between the two moieties, one of which acts as a donor (D) and the other as an acceptor (A).[6−10] A significant body of the experimental and theoretical works exist on an impressive array of systems with a rigid, semirigid, or flexible bridge between the donor and the acceptor.[11−13] It has been well established that not only the photophysical properties of the two chromophoric moieties but also the characteristics of the bridge determine the kind of interaction between the excited state of the donor moiety and the ground state of the acceptor moiety or vice versa.[14−18] One consequence of having rigid bridging systems between the donor and the acceptor moieties has been the observation of significantly enhanced energy- or electron-transfer efficiencies and rates as compared to those of nonlinked or flexibly bridged compounds.[19]

In many molecular and biological systems, intramolecular electron and energy-transfer processes occur alongside one another.[20−23] Frequently, they offer independent competing pathways for the excited state deactivation. In certain instances, they are linked together as the crucial steps of the same photoconversion chain. For example, in photosynthetic reaction centers, the elaborate antenna chromophores collect electronic energy and rapidly transfer it to the charge-separation site. The formal link between these two phenomena comes from the fact that both these processes can be viewed as the special cases of nonradiative decay of the electronic excited states and the rate of both the processes can be described by a Fermi Golden Rule formalism, which involves an electronic coupling term and a nuclear term.[24] The electronic coupling term consists of the direct donor−acceptor interaction as well as the component mediated by the intervening material, such as a bridge or the solvent. The nuclear term describes the effect of temperature, isotope, activation energy, the free energy change of the reaction, and solvation. It has been shown earlier that different solvent mediums can be used to tune the reaction mechanism between the electron and energy transfer in the same molecular system.[23]

The challenge in designing molecular systems for a particular application is to minimize the undesirable side reactions. For example, in photogalvanic cells, the efficiency of the photoin-

† Part of the special issue "Richard Bersohn Memorial Issue".

* To whom correspondence may be addressed. E-mail: dkpalit@apsara.barc.ernet.in. Tel.: 91-22-25595091. Fax: 91-22-25505151/25519613.

‡ Bhabha Atomic Research Centre.

§ University of Hyderabad.

10.1021/jp049309l CCC: $27.50
Published on Web 05/07/2004

duced electron-transfer reaction is determined by both the back electron-transfer reaction between the charge-separated states as well as the energy transfer from the donor to the acceptor, which wastes the energy of the absorbed photon. On the other hand, energy transfer also has significant applications in biological systems,[25] energy-transfer dye-laser (ETDL) operation,[26] photodynamic therapy,[27] photochemical synthesis,[28] light harvesting,[29] and many others. In these applications, the presence of electron-transfer interaction is not desirable for obtaining the maximum efficiency of the system.

The necessary condition for an intramolecular electronic energy-transfer (intra-EET) process is that the two moieties should possess the spatial configuration and spectral properties favorable for the process.[11,30] For energy transfer between the donor and the acceptor moieties in a bichromophoric molecule of the type D−A, the initial state, D*−A, should be in or near resonance with the final state, D−A*, with a suitable spatial orientation with respect to each other. Many reports are available in the literature on the studies of intra-EET processes in bichromophoric molecules, in which the donor and acceptor molecules are linked by saturated hydrocarbon bridges of varying lengths and structures.[11,12,17,18,31,32] Such flexibly bridged molecules exist in solution in different conformations having different spatial orientations between the two constituent chromophoric moieties in the molecule. Thus, the rate of the intra-EET process is an average over those due to the ensemble of molecules having different conformations. For example, Hassoon et al. reported studies on the intra-EET processes in a series of bichromophoric molecules, in which a phenyl group as the donor is connected to a dione as the acceptor moiety by $-(CH_2)_n-$ linkers.[11] The authors have explained the dependence of the efficiency of the intra-EET process on the structure of the bridge by suggesting a Dexter-type exchange interaction responsible for the same process. Temperature dependence of the intra-EET rate has been attributed to the conformational factors. Getz et al. also have reported the temperature dependence of the intra-EET process in a bichromoiphoric system of the type phenanthrene $-(CH_2)_n-$ dione.[31] However, the observed temperature dependence has been attributed to the participation of higher vibrational levels in the intra-EET process. Recently, Levy and Speiser, in a novel study, have calculated the rate of the intra-EET process in a bichromophoric molecule and showed that the rate is not only influenced by the average interchromophoric distance but also by the entire molecular geometry.[18] These authors have suggested that at small interchromophoric separation, $R < 4$ Å, Dexter's simplified approach is unable to account for the rate of the intra-EET process, which needs correction for the contributions from the relative orientations of the two chromophoric units.

We have synthesized a series of bichromophoric molecules, in which the anthracene moiety has been linked to differently modified phenanthroline moiety either by one or more σ bonds or by flexible $-CH_2-$ bridges. We observe that interchromophoric interaction in these molecules has been specific to the structure of the individual chromophores and the kind of bridge used to link them. In this paper, we present the results of our studies on the intra-EET process in a prototype bichromophoric molecular system of this series, namely, 2-(9-anthryl)-1H-imidazo [4,5-f] [1,10]-phenanthroline (AIP), where the donor and acceptor moieties are linked by a single σ bond without any intervening molecular bridge (Chart 1). The dynamics, that follows photoexcitation at the longest wavelength band of the absorption spectrum of AIP, reveals that the energy transfer from the AN moiety to the 1H-imidazo [4,5-f] [1,10]-phenanthroline

CHART 1

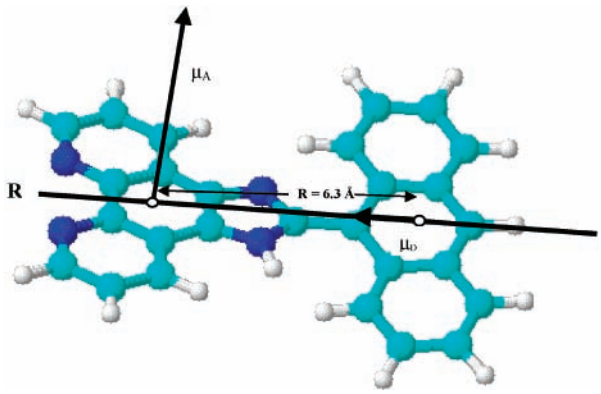

(IP) moiety is the dominant process in the excited singlet (S_1) state of the molecule. The rate of the intra-EET process follows either R^{-6} or $\exp(-R)$ dependence, depending on the mechanism of interaction responsible for the intra-EET process.[11,17,18] In the limiting case of the lowest interchromophoric separation possible, i.e., for a directly linked donor−acceptor molecular system, an ultrafast EET rate is expected. This molecule, in which the donor and acceptor moieties have planar and rigid molecular structures and separated by a minimum distance possible in a bichromophoric molecular system, offers us an excellent opportunity for investigating the dependence of intra-EET dynamics on molecular coformations.

2. Experimental Section

2.1. Materials. Anthracene obtained from Sigma Chemical Co. was used after recrystallization from methanol. All the solvents used were of spectroscopic grade (Spectrochem, India) and used as received without any further purification. High purity grade nitrogen gas (Indian Oxygen, purity >99.9%) was used to deaerate the samples.

AIP (Chart 1) and IP were synthesized by the following methods. 1,10-Phenanthroline-5,6-dione (phen-dione) was prepared by using the method already reported in the literature.[33] IP was prepared by refluxing a mixture of phen-dione (0.53 g, 2.5×10^{-3} mol dm^{-3}), formaldehyde (0.26 mL of 36−38% solution, 3.5×10^{-3} mol dm^{-3}), ammonium acetate (3.88 g, 5.0×10^{-2} mol dm^{-3}), and glacial acetic acid (7 mL) for 1 h by adopting the Steck and Day method[34−36] (yield = 0.29 g, 51%). Replacing formaldehyde with 9-anthraldehyde in the above preparation yielded AIP. The complete characterization of AIP will be published elsewhere.[37]

2.2. Instruments and Methods. Steady-state absorption spectra were recorded using a Shimadzu model UV-160A spectrophotometer. Fluorescence spectra were recorded using a Hitachi model 4010 spectrofluorimeter. The fluorescence yields were determined by comparing the areas under the fluorescence curves with those of Anthracene in ethanol (0.27) under the same experimental conditions.[38]

Three different time-resolved techniques were used to study the dynamics of the excited state. The fluorescence lifetimes were measured using a time-correlated single photon counting spectrometer (Edinburg Instruments, U.K., Model FL-199) with 1-ns time resolution. Samples were excited at 380 nm using a hydrogen-discharge flash lamp providing pulsed light output with 1-ns full width at half maximum (fwhm).

The transient absorption spectra with 35-ps time resolution were recorded using a picosecond laser flash photolysis apparatus, the details of which have been described elsewhere.[39] Briefly, the third harmonic output (355 nm, 5 mJ) from an active

passive mode-locked Nd:YAG laser (Continuum, model 501-C-10) providing 35-ps pulses was used for excitation, and the continuum (400−950-nm) probe pulses were generated by focusing the residual fundamental in a 10-cm cell containing a H2O/D2O mixture. The probe pulses were delayed with respect to the pump pulses using a 1-m linear translation stage, and the transient absorption signal at different probe delays (up to 6 ns) were recorded using an optical multichannel analyzer (Spectroscopic Instruments, Germany) interfaced to an IBM-PC. The zero delay position was assigned to that when the probe light reached the sample just after the end of the pump pulse.

Relaxation processes faster than 50 ps were measured using a femtosecond pump−probe transient absorption spectrometer. The pulses of 6 nJ of energy at 800 nm were obtained from a self-mode-locked Ti−Sapphire laser oscillator, which was pumped by a 5-W diode-pumped solid-state laser. These pulses were amplified to generate 50-fs laser pulses of about 250 μJ energy using the chirped pulse amplification technique, consisting of a pulse stretcher, a Nd:YAG laser pumped multipass amplifier, and a pulse compressor. Pump pulses for excitation of the sample at 400 nm were generated by frequency doubling of one part of the 800-nm output of the amplifier in a 0.5-mm BBO crystal and another part was used to generate the white light continuum (470−1000 nm) in a 2-mm thin sapphire plate for probing the absorption of the transient intermediate species. The sample solutions were kept flowing through a quartz cell of 1-mm path length. The polarization of the pump beam was kept at the magic angle, and the energy of this beam was maintained at about 5 μJ. The decay dynamics at a particular wavelength region (10 nm width) were monitored using two photodiodes coupled with the boxcar integrators, and the time-resolved transient absorption spectra were constructed from the temporal absorption profiles recorded at different wavelengths. The overall time resolution of the absorption spectrometer was determined to be about 120 fs by measuring the growth of the $S_1 \rightarrow S_n$ absorption of perylene in acetonitrile solution at 690 nm.

3. Results and Discussion

3.1. Ground-State Absorption and Steady-State Emission Studies. The ground-state optical absorption spectra of AIP, IP, AN, as well as an equimolar mixture of IP and AN, dissolved in methanol, are shown in Figure 1. The absorption spectrum of the equimolar mixture of AN and IP (curve "c") is simply the resultant of addition of the individual spectra of IP (curve "b") and AN (curve "a"), recorded with the same concentrations as those used in the mixture. This confirms that no intermolecular interaction exists between IP and AN in a solution of their equimolar mixture. However, for the absorption spectrum of AIP (curves "d" and "e"), in which the IP and AN moieties are linked together by a single σ bond, we observe bathochromic shifts as well as spectral broadening of the vibronic bands, which are characteristic of the individual moieties. Particularly, the line shapes of the vibronic bands characteristic of the AN moiety are significantly changed due to broadening, and also the position of each of these vibronic transitions are redshifted by about 10 nm in the absorption spectrum of AIP. Apparently, these observations may suggest some kind of electronic interaction, such as a charge-transfer or mesomeric interaction, between the two chromophoric units. However, it is observed that the positions and shapes of the vibronic bands of AIP in the 320−400-nm region are not dependent on the polarities of the aprotic solvents, such as ethyl

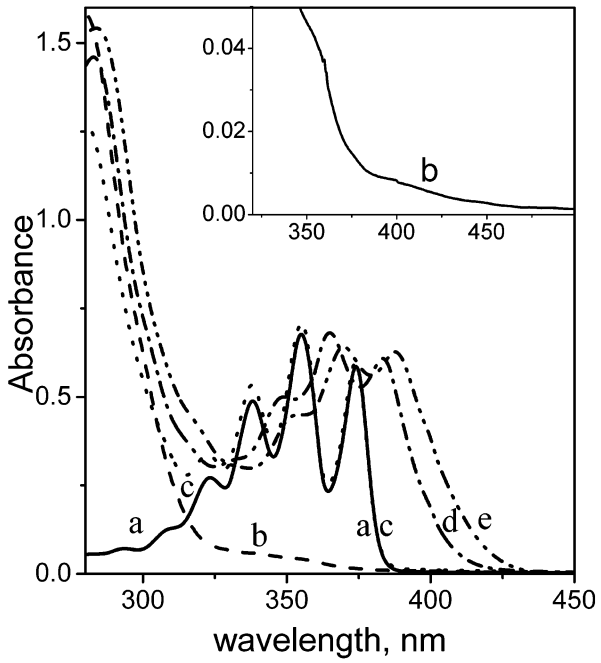

Figure 1. Absorption spectra of AN (a), IP (b), and a 1:1 mixture (by molar concentration) of AN and IP (c) in methanol along with those of AIP in methanol (d) and DMSO (e).

acetate (dielectric constant, $\epsilon = 9$), acetonitrile ($\epsilon = 37.5$), and DMSO ($\epsilon = 47$). These observations have prompted us to exclude the possibility of the charge-transfer (CT) kind of interaction, which is expected to become more prominent in more polar solvents, between the two moieties. On the other hand, a small blueshift in the positions of these vibronic bands by a few nm is noticed in alcoholic solvents, possibly due to the effect of intermolecular hydrogen bonding of AIP with alcohols.

The peak positions of the vibronic bands of AIP, which are characteristics of the anthracene moiety, have been compared with those of methylanthracene and are seen to match well within a nm.[40] The shifts in peak positions of the vibronic bands in methylanthracene compared to those in anthracene could possibly be rationalized in terms of the positive inductive effect of the methyl group.[41,42] Accordingly, the positive inductive effect of the IP moiety could possibly be the main reason for the redshift of the vibronic bands of AIP as compared to those of anthracene.

However, while the line shapes of the vibronic transitions in the isolated AN molecule have sharp Lorentzian profiles with a fwhm of ~780 cm^{-1}, the line shapes, which are characteristic of the AN moiety in AIP, deviate from the Lorentzian profile with the width increasing to 1760 and 1990 cm^{-1} in methanol and DMSO, respectively. These observed changes in the absorption spectra give strong evidence for inhomogeneous spectral broadening, which may have arisen due to either of two reasons. One of them is a weak mesomeric interaction between the two moieties and the other is that expected to be induced by the conformational flexibility of the molecule and the resulting thermal distribution of conformers in solution. Mesomeric interaction between the two moieties in a bichromophoric molecule is significant when the molecular planes of two moieties are parallel to each other.[43] Our AM1 level calculation using GAMESS software shows that the most probable twisting angle between the molecular planes of the two individual moieties is about 15°, which minimizes the steric interaction between them.[44] So, the inhomogeneous broadening of the

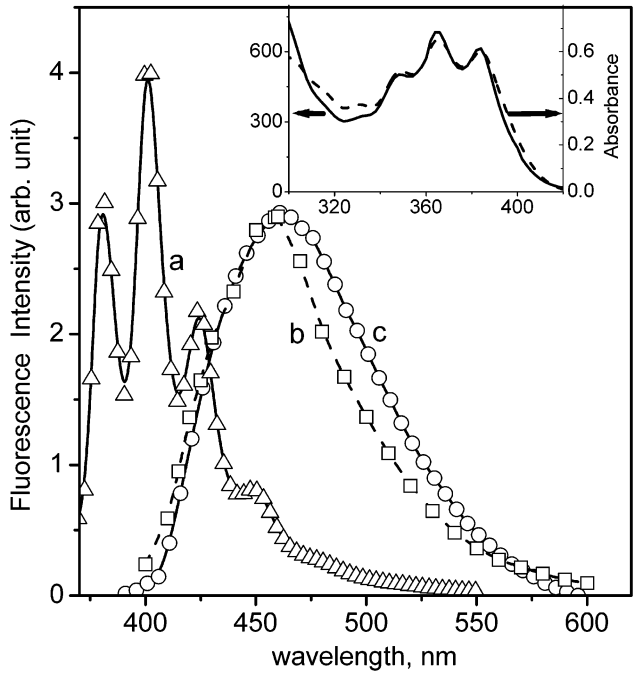

Figure 2. Fluorescence spectra of AN (a), IP (b), and AIP (c) in methanol at room temperature (excitation wavelength is 380 nm). Inset: Absorption (dashed line) and fluorescence excitation (solid line) spectra of AIP in methanol (emission wavelength is 470 nm).

vibronic bands in AIP may possibly be explained by distribution of molecular conformations having different twist angles. Hence, these arguments establish that the electronic interaction between the two moieties in the ground state of AIP should be very weak.

The fluorescence spectra of AN, IP, and AIP in methanol due to photoexcitation at 380 nm are shown in Figure 2. The fluorescence spectrum of AN (curve "a") has the typical well-defined vibronic structures. However, IP has a broad and structureless emission band, with maximum at 460 nm (curve "b"). It is interesting to note that the fluorescence spectrum of AIP (curve "c") is very similar to that of IP, although the spectral width of the former is a little broader. However, the fluorescence spectrum of AIP has no signature of the vibronic bands, which are characteristic of AN fluorescence. Spectral shape and the maximum of the fluorescence band of AIP are not sensitive to solvent polarity. In addition, the excitation profile for the emission collected at 475 nm, which corresponds to the fluorescence emission maximum of both IP and AIP, resembles well with the absorption spectrum of AIP (inset of Figure 2). These observations suggest that some of the excitation energy initially deposited into the excited-state orbitals localized on the anthracene moiety migrates to the excited-state orbitals localized on the IP moiety. Inset of Figure 1 shows that the absorption spectrum of IP has a weak absorption band near 400-nm region, suggesting that the energy of the S_1 state of IP is lower than that of AN. The absence of dual emission or complete absence of emission bands characteristic of the AN moiety in the emission spectrum of AIP, indicates a very efficient nonradiative transfer of energy from the AN moiety to the IP moiety. Additionally, the quantum yields of fluorescence of IP (0.25) and AIP (0.23) in methanol are nearly equal, indicating that the transfer of excitation energy is nearly quantitative. Additionally, other nonradiative relaxation processes undergone by the excited AN moiety leading to the ground state of AIP should have a very small contribution. The fluorescence lifetimes of AIP and IP in methanol, determined by the time-correlated single photon counting (TCSPC) technique ($\lambda_{exc} = 380$ nm and $\lambda_{em} = 500$ nm), have been found to be nearly the same (2.5 ns). The identical fluorescence lifetimes of AIP and IP confirms that the fluorescence emission from AIP is due to the radiative de-excitation process, taking place from the S_1 state of the IP moiety to the ground state of AIP.

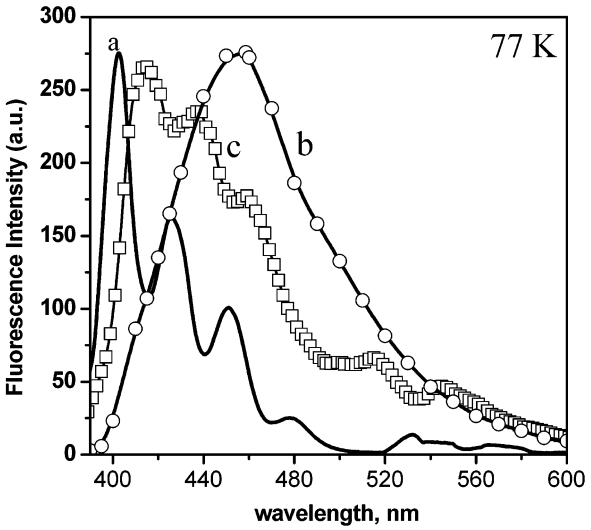

Figure 3. Emission spectra of AN (a), IP (b), and AIP (c) in a methanol glass matrix at 77 K.

We also made an attempt to observe the intermolecular energy transfer from AN (donor) to IP (acceptor) in solution using the method of steady-state quenching of fluorescence of AN. However, possibly due to limitation of solubility ($<10^{-4}$ mol dm^{-3}) of IP in any kind of solvents, polar or nonpolar, we could not observe the quenching of fluorescence of AN even with the highest concentration of IP obtainable in solution and hence no indication of the intermolecular energy-transfer process could be obtained.

Since AIP is a flexible molecule that can adopt different molecular conformations with different twist angles between the two moieties, we were interested to know whether the intra-EET process in this molecule requires any specific conformational geometry of this molecule. We have studied the emission characteristics of AIP and its individual chromophoric components in methanol glassy matrix at 77 K. In a rigid glass matrix, the molecular motions are frozen and hence no conformational change is expected to take place in the excited state. Figure 3 shows that the basic features of AN and IP emission at 77 K are very similar to those observed in their individual emission spectra recorded at room temperature. However, the emission characteristics of AIP in the glass matrix at 77 K are remarkably different from those observed in its room-temperature emission spectra (Figure 2). A comparison of the low-temperature emission spectra of AN, IP, and AIP suggests that, in the rigid matrixes, the AIP emission spectrum has the major contribution from the emission originating from the excited anthracene moiety with a minor contribution from the emission due the excited state of IP moiety. It is also important to note that the positions of the vibronic bands in the low-temperature emission spectrum of AIP correspond well with those of methylanthracene.[39] Considering the possibility that both the AN and IP moieties of AIP are photoexcited at 380 nm (see section 3.2.2), the low-temperature emission spectrum of AIP suggests either or both of the following two possibilities. One is that, following independent photoexcitation, the two moieties emit independently without any kind of interaction (say, energy transfer) between them. The other is that a fractional amount of excitation energy is transferred intramolecularly from the excited AN

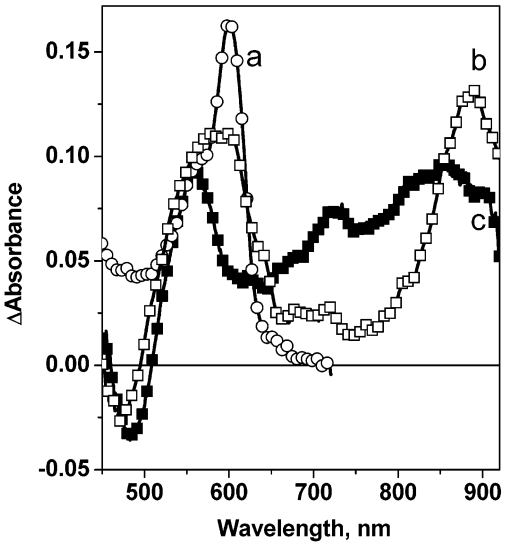

Figure 4. Transient absorption spectra of AN (a), IP (b), and AIP (c) in methanol, observed immediately after the photoexcitation with 355-nm laser pulses of 35-ps duration.

moiety to the IP moiety. Hence, in the rigid matrixes at 77 K, we observe "dual emission" from AIP. In any case, a comparison between the emission spectrum of AIP recorded at room temperature and that at low temperature clearly reveals that the efficiency of the intra-EET process in the rigid glass matrix decreases significantly as compared to that at room temperature. The higher efficiency of the intra-EET process in AIP in solutions at room temperature suggests that the molecule is required to attain a specific conformational geometry, which is suitable for efficient energy transfer, by undergoing a conformational relaxation process via twisting about the single bond connecting the two moieties.[4,10,13] Since the conformational relaxation process is inhibited or slowed significantly in rigid matrixes at 77 K, the energy-transfer process is also slowed as compared to the decay rate of the S_1 state of AN. It should be noted in this regard that the higher energy-transfer rate at room temperature could also be explained by assuming the participation of higher vibrational levels. At room temperature, the vibrationally excited states of the donor become populated and an efficient vibronic coupling with those of the acceptor may enhance the efficiency of the energy-transfer process.[31,45] To address these questions and to have better understanding about the energy-transfer mechanism, detailed transient absorption studies have been carried out on AIP, the results of which are presented below.

3.2. Transient Absorption Studies. *3.2.1. Transient Absorption in the Picosecond Time Domain.* Figure 4 shows the transient absorption spectra of AIP, AN, and IP in methanol, obtained immediately after photoexcitation with 355-nm laser pulses of 35-ps duration. In the case of AN, the transient absorption spectrum (spectrum a) consists of an absorption band in the 500−650-nm region with maximum at ca. 600 nm and a shoulder at ca. 580 nm. This could be assigned to the $S_n \leftarrow S_1$ transition in AN following the earlier report.[46] In the case of IP, the transient absorption spectrum (spectrum b) consists of two absorption bands in 500−675 nm and 800−900 nm region, with maxima at ca. 590 and 875 nm, respectively. This spectrum also shows a weak absorption shoulder at ca. 700 nm and a weak stimulated emission band in 450−500-nm region. All these bands in the transient absorption spectrum of IP (spectrum b) in the entire 450−950-nm region could be assigned to the S_1 state of IP. This interpretation is supported by the fact that the

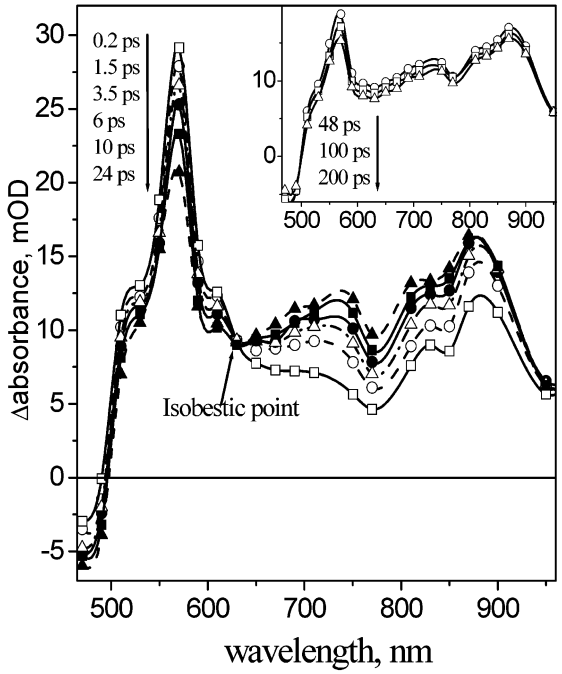

Figure 5. Transient absorption spectra of AIP in methanol, recorded at different delay times (longer delay times are shown in the insets) following photoexcitation with 400-nm laser pulses of 50-fs duration.

lifetimes, which have been determined from the temporal absorption profiles monitored at 470, 590, and 850 nm, are nearly the same (∼2.5 ns) as those determined by the fluorescence lifetime measurements (vide supra).

The transient absorption spectrum of AIP in methanol (spectrum "c") shows nearly the similar spectroscopic features as those observed in the S_1 state spectrum of IP (spectrum "b"). This observation suggests that the excitation energy supplied to the AN moiety due to photoexcitation of AIP at 400 nm is transferred to the IP moiety within a 35-ps time domain. However, we also observe a few distinct differences between the spectra "b" and "c". The absorption maximum seen at 590 nm in the S_1 state spectrum of IP has been shifted to 570 nm in that of AIP, and the width of the latter is considerably reduced. On the other hand, the S_1 state absorption band of AIP in 700−920-nm region has been considerably broadened and the maximum has been shifted to 850 nm as compared to that at 900 nm in the absorption spectrum of the S_1 state of IP. These differences in the spectral features of the absorption spectra of the S_1 states of IP and AIP indicate stronger electronic interaction between the AN and IP moieties in the S_1 state of AIP.

3.2.2. Transient Absorption in the Femtosecond Time Domain. The time-resolved transient absorption spectra of AIP in methanol recorded in the femtosecond time domain, following photoexcitation with 400-nm laser pulses of 50-fs duration, are shown in Figure 5. The spectrum recorded at 0.2 ps after photoexcitation of AIP shows a strong and sharp absorption band in the 510−610-nm region with a maximum at ca. 570 nm and a shoulder at 530 nm. Another weak but very broad absorption band in the 650−950-nm region as well as a weak stimulated emission band in the 470−500-nm region were also seen (470 nm is the shortest wavelength up to which we are able to monitor the transient absorption or stimulated emission signal using our spectrometer). The time-resolved transient spectra recorded up to 210 ps show that, while the absorbance in the 510−610-nm region continuously decays, the stimulated emission band in 470−500-nm region and the absorption band

in the 650−950-nm region grow initially with increase in time delay up to about 24 ps and then start decaying at the longer delay times (inset of Figure 5). The temporal absorption profiles measured at different wavelengths within the same absorption or the stimulated emission band have been found to follow nearly similar kind of dynamics. Additionally, we observe the presence of a well-defined isobestic point at 630 nm, which is retained up to the 24-ps time domain. This observation suggests that the transient species having an absorption band in the 650−950-nm region and the stimulated emission band in the 470−500-nm region grow at the expense of the decay of the transient species having an absorption band in the 510−610-nm region. Considering the positions of the bands in the S_1 state absorption spectra of IP and AN, both the absorption band in the 650−950-nm region as well as the stimulated emission band in the 470−500-nm region in the transient spectrum of AIP recorded at 0.2 ps could be assigned to the S_1 state, for which the energy is localized on the electronic orbitals of the IP moiety. The other absorption band in the 510−610-nm region with a maximum at 570 nm in the same spectrum may have contribution from the S_1 state absorption due to both the AN and IP moieties. Comparing the relative absorbance values at 850 and 570 nm in the S_1 state absorption spectra of IP and AIP (spectrum "b" and "c", respectively, in Figure 4), it becomes obvious that, in the transient absorption spectrum of AIP recorded at 0.2 ps, the absorbance at 570 nm has a negligible contribution from the S_1 state absorption due to the IP moiety but the major contribution from the S_1 state absorption due to the AN moiety. Hence, the evolution of the time-resolved absorption spectra, as shown in Figure 5, could be explained by the decay of the S_1 state absorption of the AN moiety at 570 nm and concomitant growth of the S_1 state absorption of the IP moiety in the 650−900-nm region because of energy transfer from the excited AN moiety to the unexcited IP moiety.

We have shown three typical temporal absorption profiles recorded at 490, 570, and 830 nm in methanol in Figure 6. Since, only the S_1 state of the IP moiety absorbs at 830 nm, at which the S_1 state of the AN moiety has negligible absorption, the temporal evolution at this wavelength provides a clear understanding about the early-time excited-state dynamics of AIP. The origin of the three distinct time domains, which are of importance in the temporal absorption profiles recorded at 830 nm, have been identified and explained as follows:

Region I: An initial growth of the transient absorption with the instrument response time (125 fs) possibly arises due to either direct excitation of the IP moiety in AIP or an ultrafast component of energy transfer. Although the ground state of the isolated IP molecule has a very weak absorption at 400 nm ($\epsilon = 700$ dm^3 mol^{-1} cm^{-1}) due to the nπ* forbidden transition, because of the electronic interaction between the two moieties in AIP, the oscillator strength of this transition may have been increased, making direct excitation of the IP moiety possible. Another possibility is that, in the case of a strong-coupling between the two chromophoric units in a bichromophoric molecule, an ultrafast component of coherent energy transfer with decay time constants of about a few tens of a femtosecond has been observed in a few cases.[47] However, in our case, due to the longer instrument response time, it has not been possible to resolve this component but possibly has appeared as a very fast initial growth of the S_1 state absorption of IP with the instrument response time. Transfer of a fractional amount of energy even in rigid matrixes may possibly be the consequence of the coherent transfer of energy from the AN moiety to the IP moiety.

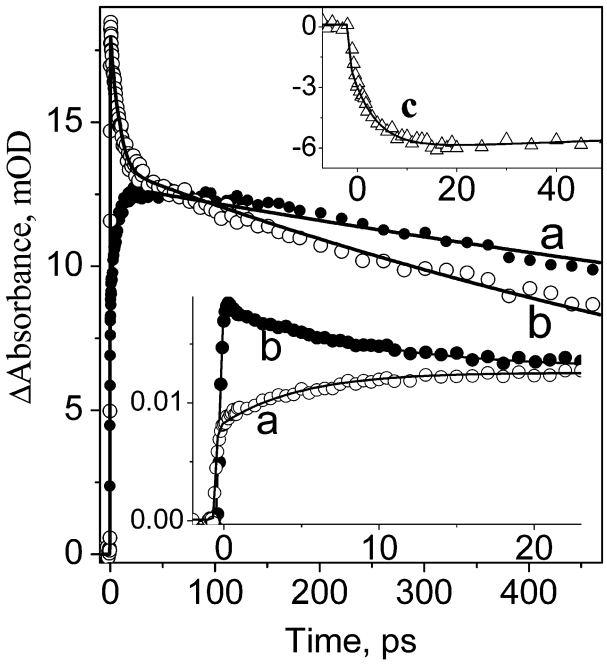

Figure 6. Temporal absorption profiles recorded at 830 nm (a) and 570 nm (b) and stimulated emission profile recorded at 490 nm (c) following photoexcitation of AIP in methanol with 400-nm laser pulses of 50-fs duration. Each point is averaged over 2000 measurements. Solid lines are the exponential fit function deconvoluted with the Gaussian instrument response function of 125-fs full width at half maximum. The profile "a" has been fitted with three components: one ultrafast growth component ($\tau_g = 125$ fs) and another slower growth component ($\tau_g = 5.1$ ps) and a long decay component ($\tau_d > 1$ ns). The absorption profile "b" has been fitted with a multiexponential function having four components: one ultrafst decay component ($\tau_d \approx 100$ fs), one decay and one growth components of equal lifetime (($\tau_d = \tau_g = 5.1$ ps), and another long decay component ($\tau_d > 1$ ns). The stimulated emission profile, "c" has been fitted with a growth component with the lifetime of 4.8 ps and a long decay component with >1 ns lifetime.

Region II: Subsequent growth of the transient absorption with a 5.1-ps growth lifetime is ascribed to the formation of the S_1 state of the IP moiety due to the incoherent transfer of the excitation energy localized on the AN moiety to the unexcited IP moiety. The growth lifetime of 5.1 ps in methanol indicates a very rapid process of energy transfer (the rate of the the energy-transfer process $k_{EET} = 1.8 \times 10^{11}$ s^{-1}).

Region III: A very long decay component (lifetime > 1 ns), which represents the decay of the S_1 state of AIP, in which the excitation is localized on the IP moiety by radiative and/or nonradiative processes leading to the ground state.

These observations and analyses are further corroborated by the results of the analysis of the decay dynamics monitored at 490 and 570 nm. Stimulated emission monitored at 490 nm, which is characteristic of the IP moiety, grows with about a 4.8-ps lifetime and decays with >1-ns lifetime. This observation supports the idea of the intra-EET process from the excited AN to the unexcited IP moiety. The transient absorption dynamics monitored at 570 nm, at which the S_1 states of both AN and IP chromophores absorb (spectra "a" and "b", respectively, in Figure 4), is expected to show an instrument-limited rise of absorption, which should be followed by a complex multiexponential dynamics consisting of the components due to the decay of the excited AN moiety, the growth of the excited IP moiety, as well as the decay of the S_1 state of AIP to the ground-state. Hence, the temporal absorption profile recorded at 570 nm has been fitted with an instrument-limited rise of absorption and three other exponential functions, which are one decay and

one growth components, both of them having nearly equal lifetimes of 5.1 ps, as well as another decay component of lifetime longer than 1 ns (Figure 6). The appearance and maintenance of the isobestic point at ~630 nm up to 24 ps also indicates the involvement of a single precursor → successor type process and no other channels of comparable rate in the ultrafast excited-state dynamics of AIP. All these experimental observations confirm intramolecular transfer of excitation energy from the AN moiety to the unexcited IP moiety following photoexcitation of AIP with 400-nm light. It is important to note that the excited singlet-state absorption due to the isolated AN moiety does not show any decay at 570 nm within 100 ps, since the S_1 state lifetime of AN is about 4.7 ns in methanol.[38] This shows that the excited AN moiety in AIP has a very fast nonradiative decay channel, which is not observed in the isolated AN molecule.

3.2.3. Effect of Viscosity. The absence or very low efficiency of the intra-EET process in a glass matrix at 77 K, in which the molecular motions are nearly frozen, suggests that the same process may require a particular conformation, i.e., a particular spatial orientation between the two moieties in the molecule. To substantiate further the requirement of attaining the preferred conformational geometry for an efficient intra-EET process, the growth lifetimes of the transient absorption signal at 830 nm was measured in a series of normal alcoholic solvents and DMSO, varying the viscosity of the medium. Because of the limitation of solubility of AIP in other kinds of solvents, femtosecond transient absorption experiments could be performed only in alcohols and in DMSO. The growth lifetime of the transient absorption measured at 830 nm, which provides the rate of formation of the S_1 state of IP moiety due to energy transfer from the excited AN moiety, becomes longer with increasing viscosity of the solvents. This implies that the rate of intra-EET process slows down in solvents of higher viscosity. This viscosity dependence suggests that attainment of a particular conformational geometry in the S_1 state in AIP via diffusive rotation of the molecular planes of the individual chromophoric moieties about the σ bond connecting them is a necessary requirement for an efficient intra-EET process.

An attempt has been made by us to find a correlation between the rates of the intra-EET (k_{EET}) process as a function of viscosity of the solvents. The most widely used model for the description of isomerization or conformational relaxation dynamics is that of Kramers.[48] The combination of his ideas with the recent calculations and the experimentally observed facts led to the formulation of an empirical power law expression, which fits all the data for the rate constants of isomerization and conformational changes and can be written in the form of eq 1[49,50]

$$k_{iso} = \left(\frac{B}{\eta^a}\right) \exp\left(-\frac{E_{act}}{RT}\right) \qquad (1)$$

The two factors in this functional form represent the contributions of two different factors controlling the isomerization or conformational relaxation rate. The first factor (i.e., B/η^a, where B is a constant, and $0 \le a \le 1$) is a universal function of viscosity and represents the "friction" or "dynamical" effects exerted by the surrounding solvent or medium opposing the motion of the parts of the molecule involved in the conformational relaxation process. The second factor, $\exp(-E_{act}/RT)$, represents the "barrier" or "static" effects represented in the form of activation energy for the conformational relaxation. The height of the energy barrier mainly depends on the nature of solute−solvent interaction. At a particular temperature and if E_{act} remains more or less unchanged in different kinds of solvents, the exponential term may be considered as a constant factor. Hence eq 1 may be written as

$$\ln(k_{iso}) = a \ln(1/\eta) + C \qquad (2)$$

A plot of $\ln(k_{iso})$ vs $\ln(1/\eta)$ should be a straight line with a positive slope having a value equal to "*a*" and the intercept is equal to the constant, $C = \ln(B) - E_{act}/RT$.

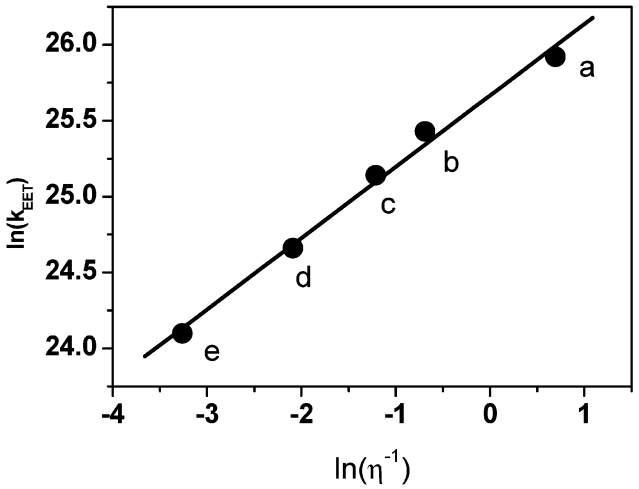

Figure 7. Plot of $\ln(k_{EET})$, the natural logarithm of the rate of energy transfer (inverse of τ_g determined at 830 nm), vs $\ln(\eta^{-1})$, the natural logarithm of the inverse of the bulk viscosity of the solvents (eq 2 in the text). The solvents in which the growth lifetimes have been measured are (a) methanol (5.1 ps), (b) dimethylsulfoxide (9 ps), (c) butanol (12 ps), (d) octanol (19.5 ps), and (e) ethylene glycol (35 ps). The least-squares fit line drawn through the data points has the slope $a = 0.47$.

Figure 7depicts the plot of the natural logarithm of the rate constants, k_{EET} ($1/\tau_g$), which have been determined by monitoring the growth of the transient absorption at 830 nm following photoexcitation of AIP in different solvents as a function of the natural logarithm of the inverse of bulk viscosities of the corresponding solvents. The plot shows a good linear correlation between the two parameters. The viscosity dependence of k_{EET} indicates that the efficiency of the energy-transfer process is guided by the conformational change in the excited state of AIP and that this rate of conformational change is the rate-determining step for the ET process. Fleming[49] and Waldeck [50] made attempts to find out a correlation between E_{act} and the parameter "*a*" through a careful investigation of the results reported from the numerous studies performed on the isomerization reactions and conformational relaxation processes. A few important points have emerged from these investigations. The most important one, which is relevant to our studies, is that, in case of a small barrier for the conformational relaxation process, the rate for the same has strong dependence on the viscosity of the solvents. The value of "*a*", which can be determined from the slope of the best fit straight line, can be a rough measure of the barrier height. A moderate value of "*a*" (0.47) obtained in this case indicates the existence of a moderate energy barrier for conformational relaxation in AIP. A linear viscosity dependence of the energy-transfer rate also reveals that the conformational relaxation process, which is strongly coupled to the intra-EET process, is mainly guided by the dynamical solvent viscosity effects. This observation is also important to conclude that the efficiency of the energy-transfer process is sensitive only to conformational changes and not to vibronic

interactions, i.e., the higher efficiency of this process at room temperature as compared to that at 77 K is not due to vibronic coupling between the higher vibrational levels of the donor and the acceptor moieties.[31,45]

3.4. Quantum Efficiency of Energy Transfer. The quantum efficiency, Q, of the intra-EET process is given by eq 3[18a]

$$Q = (k_{EET}/(k_{EET} + k_f)) \tag{3}$$

Considering the value of k_{EET} obtained in methanol ($k_{EET} = 1.8 \times 10^{11}$ s^{-1}) and the lifetime of anthracene in methanol (4.7 ns),[38] and hence $k_f = 2.13 \times 10^8$ s^{-1}, the value of Q could be calculated to be nearly unity. This indicates a very efficient intra-EET process in AIP in methanol at room temperature. In other solvents, too, the process is equally efficient at room temperature.

3.5. Mechanism of Energy Transfer. The results discussed above indicate that, following photoexcitation, AIP undergoes a very fast and efficient intra-EET process (the rate of energy transfer varies from 3×10^{10} s^{-1} to 18×10^{10} s^{-1} in different solvents, and efficiency is near unity). However, it is important to know the mechanism of energy transfer and to delineate the kind of interaction between the two chromophoric units, which is a key factor in the intra-EET process. We observe two distinct components of the intra-EET process following photoexcitation of AIP. The ultrafast component, which takes place within the instrument response time (~120 fs), indicates a coherent excitonic mechanism due to the strong electronic interaction between the dipoles of the two moieties in the S_1 state of AIP.[47] The slower component, the rate of which shows strong viscosity dependence, represents the incoherent component of the energy-transfer process. On the basis of the vast amount of theoretical and experimental studies on numerous kinds of chemical systems, it has been well established that the incoherent intra-EET process may follow any of the three possible mechanisms: (1) the Förster mechanism by dipole−dipole-induced (columbic) resonant interaction,[51,52] (2) the Dexter mechanism by direct through-space exchange interaction,[53] and/or (3) through-bond-mediated exchange interaction.[54,55]

Since in AIP, the donor and the acceptor moieties are linked directly to each other by only one C−C σ bond without intervention of any kind of molecular bridges, the contribution of the through-bond-mediated exchange-interaction mechanism toward the energy-transfer process should be considered negligible. Hence, the intra-EET process in this molecule should follow either the Förster mechanism and/or the Dexter mechanism, and the rate of energy transfer should be dependent upon the degree of overlap between the donor emission and the acceptor absorption spectra. The spectral overlap integrals for resonance interaction, J_{res} and exchange interaction, J_{ex}, between the AN emission and the IP absorption for the AIP molecule can be calculated using eqs 4 and 5 based on the spectral properties of the isolated AN and IP molecules

$$J_{res} = \int_0^\infty \frac{\bar{F}_D(\bar{\nu})\epsilon_A(\bar{\nu})\, d\bar{\nu}}{\bar{\nu}^4} \text{ dm}^3 \text{ mol}^{-1} \text{ cm}^3 \tag{4}$$

$$J_{ex} = \int_0^\infty \bar{F}_D(\bar{\nu})\bar{\epsilon}_A(\bar{\nu})\, d\bar{\nu} \text{ cm} \tag{5}$$

with $\bar{\nu}$ in cm^{-1}. $\bar{\epsilon}_A(\bar{\nu})$ in dm^3 mol^{-1} cm^{-1} and $\bar{F}_D(\bar{\nu})$ are the normalized absorption and emission spectra of the acceptor and donor, respectively

$$\int_0^\infty \bar{F}_D(\bar{\nu})\, d\bar{\nu} = \int_0^\infty \bar{\epsilon}_A(\bar{\nu})\, d\bar{\nu} = 1 \tag{6}$$

The values of J_{res} and J_{ex} for AIP have been calculated to be 1.9×10^{-16} dm^3 mol^{-1} cm^3 and 1.1×10^{-4} cm, respectively. The nonzero and significantly large values of both J_{res} and J_{ex} suggests the possibility that either or both of the Förster resonance and Dexter exchange interactions contribute in conjunction to the intra-EET process in AIP, although not exclusively.

In the case of resonance interaction (i.e., the Förster mechanism), the critical transfer distance, R_0, can be calculated using eq 7. R_0 represents the distance of separation between the donor and the acceptor at which the probability of energy transfer by this mechanism is equal to that of the decay of the donor

$$R_0^6 = \frac{9000 \ln(10)\kappa^2\Phi_D J_{res}}{128\pi^5 n^4 N_A} \tag{7}$$

wher ϕ_D is the fluorescence quantum yield of the donor, AN (0.27 in methanol), "n" the refractive index of the solvent (1.265 for methanol), and "N_A" the avogadro's number (6.023×10^{23} dm^3 mol^{-1}). The value of R_0 is also influenced by the orientation factor (κ^2), which depends on the angle between the transition dipole moment vectors for the donor emission and acceptor absorption. The value of κ^2 can vary from 0 to 4 depending on the relative orientation of these two vectors.[52] Most implementations of Förster's theory involve systems consisting of a donor molecule surrounded by an ensemble of randomly oriented acceptor molecules, and under these conditions (for which the theory was originally developed), the κ^2 term can often be assumed to be equal to $^2/_3$.[52] This is clearly inappropriate for bichromophoric molecules such as AIP, in which the relative orientation between the emission and absorption transition dipoles of a single donor and a single acceptor chromophore, which are linked with each other by a single σ bond, are well defined. In aromatic molecules, both the absorption and emission dipole moment vectors always lie on the molecular plane. In such cases, the orientation factor, κ, is given by eq 8[52]

$$\kappa = \sin\theta_D \sin\theta_A \cos\phi - 2\cos\theta_D \cos\theta_A \tag{8}$$

where θ_D and θ_A are the angles between the emission and absorption dipole moment vectors of the donor, μ_D, and acceptor, μ_A, where the vector **R** connects the centers of the chromophoric units and ϕ is the dihedral angle between the planes of (μ_D,**R**) and (μ_A,**R**) (Chart 1). Equation 8 suggests that κ may have different values for different molecular conformations, in which the dihedral angle, ϕ, between the molecular planes of the two chromophoric units are different.

It is known that, in the anthracene molecule, both the $S_1 \leftarrow S_0$ absorption and $S_1 \rightarrow S_0$ fluorescence emission dipole moment vectors are short-axis polarized.[56] Hence, in AIP, the emission dipole of the donor moiety lies along the molecular axis, **R**, and θ_D should be taken as 0°. Equation 8 thus can be written as

$$\kappa = -2\cos\theta_D \cos\theta_A \tag{9}$$

Equation 9 suggests that, if the energy transfer follows the Förster energy-transfer mechanism, the rate of the intra-EET process should be independent of the dihedral angle, ϕ, between the molecular planes of the donor and acceptor moieties. Now our calculation using ab initio molecular orbital theory shows that the dipole moment vector for the $S_0 \rightarrow S_1$ transition in an isolated IP molecule lies at a direction of 80° with respect to the direction of the molecular axis, **R**, and this gives the value of θ_A. Hence, the value of κ, calculated using eq 9, is −0.278

and R_0, the critical energy-transfer distance, calculated using eq 7, is 10.5 Å. If the energy transfer is exclusively due to Förster interaction, the rate of the intra-EET process, k_{EET}^{res}, can be calculated using eq 10

$$k_{EET}^{res} = (1/\tau_D)((R_0/R))^6 \quad (10)$$

where τ_D is the lifetime of the donor emission in the absence of energy transfer (the lifetime of AN in methanol is 4.7 ns).[38] In the present case, the value of R, the center-to-center distance between the AN and IP moieties in AIP, has been theoretically calculated to be about 6.3 Å. Hence, the value of k_{EET}^{res} in methanol, calculated using eq 10, is 4.6×10^9 s^{-1}. The theoretical efficiency of the energy transfer due to the Förster mechanism, Q_F, can be calculated using eq 11

$$Q_F = ({R_0}^6/{R_0}^6 + R^6) \quad (11)$$

The value of Q_F thus calculated is 0.95. This value is less than the value of Q (unity), calculated using eq 3, which defines the transfer efficiency in terms of the measured rate constants for the energy transfer and the rate of the decay of the donor emission.

Now, we observe that the parameters, calculated above on the assumption that the Förster mechanism of energy transfer is operative exclusively in AIP, show some inconsistencies with those determined from our time-resolved experiments. First, the rate calculated for Förster energy transfer in methanol ($k_{EET}^{res} = 4.6 \times 10^9$ s^{-1}) is about 2 orders of magnitude smaller than the rate ($k_{EET} = 1.8 \times 10^{11}$ s^{-1}) of the intra-EET process experimentally determined in the same solvent. Second, the efficiency of the Förster energy transfer, Q_F, is also smaller than the experimentally determined value, Q. Last, the application of Förster's theory in the case of AIP predicts no dependence of the energy-transfer rate on the dihedral angle, ϕ, between the molecular planes of the two chromophores (eq 9). The results of the time-resolved experiments suggest that the rate of energy transfer decreases linearly with increase in viscosity of the solvents. Hence the dependence of the energy-transfer rate on the viscosity of the solvents could not be explained by the Förster theory.

In addition, due to the R^{-6} dependence of the rate of the dipole−dipole-induced EET process, the Förster mechanism is predicted to be predominantly operative in longer separation distance ($R > 10$ Å) between the donor and the acceptor.[17,18] At smaller separation distances ($R < 10$ Å), the Förster formulation, which is valid only for point dipoles, gives us only a rough estimate of the EET rate. Moreover, at shorter distances of interchromophoric separation, one has to take account of exchange interaction due to overlap of donor emission and acceptor absorption orbitals (the Dexter mechanism). The rate of energy transfer by the Dexter through-space exchange-interaction mechanism can be calculated using eq 12

$$k_{EET}^{ex} = (4\pi/h)KJ_{ex} \exp(-(2R/L)) \quad (12)$$

where L is an average van der Waal radius for the initial and final molecular orbitals of the donor−acceptor system and K is a parameter that cannot be directly evaluated from the spectroscopic data and hence makes it difficult to calculate the exchange contribution to the EET rate. However, the dependence of k_{EET}^{ex} on the term $\exp(-2RL)$ suggests that this mechanism is expected to be operative at a shorter distance of separation.[17] In the case of AIP, the calculated value of R (6.3 Å) suggests the possibility of the predominance of the Dexter mechanism in the intra-EET process.

From the earlier studies on the various kinds of molecular systems, it was, however, realized that a dependence of the transfer rate on the relative orientation of the donor and acceptor must exist, particularly at small R values. Levy and Spieser performed a novel calculation of the exchange integral in a xylene−biacetyl-type of bichromophoric molecules for describing the efficiency of the intra-EET processes.[18a] It was shown that Dexter's simplified approach, which predicts an exponential dependence of the transfer rate on the interchromophoric distance, is insufficient to account for the observed experimental results and indicated a significant contribution from the relative orientation of the two chromophores.

The above arguments suggest that the observed EET in AIP is most likely not occurring by the purely Förster dipole−dipole interaction mechanism, although its contribution cannot be neglected, but rather may involve a significant contribution from the Dexter through-space exchange-interaction mechanism. We have already indicated that the significantly large value of J_{ex} (1.1×10^{-4} cm) suggests the possibility of contribution from the Dexter's exchange interaction to the EET process. Viscosity dependence of k_{EET} also suggests the contribution of the Dexter mechanism. The intra-EET process prefers a particular relative orientation of the molecular planes, which can be achieved by a conformational relaxation process following photoexcitation of AIP for efficient exchange interaction between the molecular orbitals of the AN and IP chromophoric moieties. The fastest rate of energy transfer is possible when the molecule attains a molecular configuration in which the molecular planes of the two moieties are parallel to each other to ensure the strongest interaction of the π^* and π orbitals of the AN and IP moieties, respectively. Hence the molecule needs to undergo a conformational relaxation process to bring the dihedral angle between the two molecular planes from 15° (which is the angle in the ground state of the molecule and hence in the Franck−Condon state) to 0° following photoexcitation of the molecule. In this case, the rate of the energy-transfer process is controlled by the rate of the conformational relaxation process, which involves the diffusive rotation of the two chromophoric moieties of AIP. Our experimental measurements could only provide the rate of the energy transfer limited by the rate of the conformational relaxation, and hence we possibly measured the rate of the latter process using the intra-EET process as a probe.

Conclusion

Steady-state and time-resolved absorption and fluorescence spectroscopic properties of AIP, a bichromophoric molecule, reveal that a rapid and efficient intra-EET process dominates its excited-state relaxation dynamics in solution. The rate of the energy-transfer process decreases linearly with increase in viscosity of the solvent, and the process is significantly retarded in rigid glass matrixes. These observations suggest strong coupling between the conformational relaxation and the energy-transfer process. Since the latter is favored in a particular conformationl geometry, which is different from that of the ground state, the molecule needs to undergo a conformational relaxation process.

Since the two constituent chromophoric units, AN and IP, are directly linked to each other without the presence of any kind of molecular bridging unit between them, the contribution from the through-bond exchange-interaction mechanism to the energy-transfer process should be negligible, and hence, contributions of the Förster and Dexter mechanisms of energy

transfer have been considered. The theoretically calculated energy-transfer rate by the Förster dipole−dipole-induced resonance-interaction mechanism is about 2 orders of magnitude smaller than the experimentally determined rate. Hence the contribution of the Dexter through-space exchange-interaction mechanism has been considered to be predominant in AIP. The short interchromophoric separation (6.3 Å) and requirement of specific conformational geometry for an efficient energy-transfer process support the operation of the Dexter through-space exchange-interaction mechanism in AIP. Viscosity dependence of the experimentally measured rates suggests that we possibly measured the conformational relaxation rate using the energy-transfer process as the probe.

Acknowledgment. We gratefully acknowledge the help from Dr. Tapan Ghanty of Radiation Chemistry & Chemical Dynamics Division, BARC in calculation of the absorption dipole-moment vector of IP and Dr. Chiranjib Mazumder of Novel Material & Structural Chemistry Division, BARC for theoretical optimization of the ground state geometry of AIP. We gratefully acknowledge fruitful discussion with Prof. Biman Bagchi of I.I. Sc., Bangalore on the mechanism of energy transfer in bichromophoric molecules. D.K.P. and B.G.M. are grateful to the Board of Research for Nuclear Sciences, Department of Atomic Energy, India, for financial support.

References and Notes

(1) *Molecular Electronics: Science and Technology*; Aviram, A., Ratner, M. M., Eds.; New York Academy of Sciences, New York, 1998; Vol. 852.

(2) *Electron Transfer in Chemistry*; Balzani, V., Ed.; Wiley V. C. H.: Weinheim, 2001; Vol. 5.

(3) *Molecular electronic Devices*; Carter, F. L., Ed; Dekker: New York, 1982; Vol. I.

(4) *Molecular electronic Devices*; Carter, F. L., Ed; Dekker: New York, 1987; Vol. II.

(5) Skourties, S. S.; Beratan, D. N. Theories of Structure−Function Relationships for Bridge-Mediated Electron-Transfer Reactions. In *Electron Transfer - From Isolated Molecules to Biomolecules*; Jortner, J., Boxon, M., Eds.; Advances in Chemical Physics, John Wiley: New York, 1999; Vol. 106, Part 1, p 377.

(6) Strachan, J. P.; Gentleman, S.; Seth, J.; Kalsbeck, W. A.; Lindsey, J. S.; Holton, D.; Bocian, D. F. *J. Am. Chem. Soc.* **1997**, *119*, 1191.

(7) Scholes, G. D.; Ghiggino, K. P. *J. Photochem. Photobiol., A* **1994**, *80*, 355.

(8) Scholes, G. D. *J. Phys. Chem.* **1996**, *100*, 18731.

(9) Scholes, G. D.; Ghiggino, K. P. *J. Chem. Phys*. **1994**, *101*, 1251.

(10) Harcourt, R. D.; Scholes, G. D.; Ghiggino, K. P. *J. Chem. Phys*. **1994**, *101*, 10521.

(11) Hassoon, S.; Lustig, H.; Rubin, M. B.; Speiser, S. *J. Phys. Chem.* **1984**, *88*, 6367.

(12) Levy, S. T.; Rubin, M. B.; Speiser, S. *J. Am. Chem. Soc.* **1992**, *114*, 10747.

(13) Gudipati, M. S. *J. Phys. Chem.* **1994**, *98*, 9750.

(14) Onuchic, J. N.; Beratan, D. N.; Winkler, J. R.; Gray, H. B. *Annu. Rev. Biophys. Biomol. Struct*. **1992**, *21*, 349.

(15) Onuchic, J. N.; Beratan, D. N. *J. Chem. Phys*. **1990**, *92*, 722.

(16) Newton, M. D.; Cave, R. J. *Molecular Control of Electron and Hole Transfer Processes - Theory and Applications In Molecular Electronics*; Jortner, J., Ratner, M., Eds.; Blackwell: Malden, MA, 1997.

(17) (a) Speiser, S. *Chem. Rev.* **1996**, *96*, 1953. (b) Speiser, S. *J. Photochem*. **1992**, *22*, 195.

(18) (a) Levy, S.; Speiser, S. *J. Chem. Phys*. **1992**, *96*, 3585. (b) Franzen, S.; Goldstein, R. F.; Boxer, S. G. *J. Phys. Chem.* **1993**, *97*, 3040.

(19) Speiser, S. *J. Lumin.* **2003**, *102*−*103*, 267−72.

(20) Scholes, G. D.; Ghigginho, K. P. *J. Phys. Chem*. **1994**, *98*, 4580.

(21) Closs, G. L.; Priotrowiak, P.; MacInnes, J. M.; Fleming, G. R. *J. Am. Chem. Soc*. **1988**, *110*, 2652.

(22) Stanley, R. J.; King, B.; Boxer, S. G. *J. Phys. Chem.* **1996**, *100*, 2052.

(23) Fournier, T.; Tavender, S. M.; Parker, A. W.; Scholes, G. D.; Phillips, D. **1997**, *101*, 5320.

(24) (a) Lin, S. H. *J. Chem. Phys.* **1989**, *90*, 7103. (b) Lin, S. H. *Mol. Phys.* **1971**, *21*, *853*.

(25) Conrad, R. H.; Brand, L. *Biochemistry* **1986**, *25*, 5377.

(26) Singh, R. D.; Sharma, A. K.; Unnikrishnan, N. V.; Mohan, D. *J. Mod. Opt*. **1970**, *37*, 419.

(27) Henderson, B. N.; Dougherty, T. J. *J. Photochem. Photobiol*. **1992**, *55*, 145.

(28) Weber, S. E. *Chem. Rev.* **1990**, *90*, 1469.

(29) Lamola, A. A.; Turo, N. J. *Energy Transfer and Organic Chemistry*, Benjamin: New York, 1961.

(30) Mataga, N.; Kubo, T. *Molecular Interaction and Electronic Spectra*; Marcel Dekker: New York, 1970; Chapter 5.

(31) Getz, D.; Ron, A.; Rubin, M. B.; Speiser, S. *J. Phys. Chem*. **1980**, *84*, 768.

(32) Smith, T. A.; Lokan, N.; Cabral, N.; Davies, S. R.; Paddon-Row: M. N.; Ghigginho, K. P. *J. Photochem. Photobiol., A* **2002**, *149*, 55.

(33) Yamada, M.; Tanaka, Y.; Yoshimoo, Y.; Kuroda, S.; Shimao, I. *Bull. Chem. Soc. Jpn.* **1992**, *65*, 1006.

(34) Wu, J. Z.; Ye, B. H.; Wang, L.; Ji, L. N.; Zhou, J. Y.; Li, R. H.; Zhou, Z. Y. *J. Chem. Soc., Dalton Trans.* **1997**, 1395.

(35) Wu, J. Z.; Li, L.; Zeng, T. X.; Ji, L. N.; Zhou, J. Y.; Luo, T.; Li, R. H. *Polyhedron* **1997**, *16*, 103.

(36) Steck, E. A.; Day, A. R. *J. Am. Chem. Soc*. **1943**, 452.

(37) Maraippan, M.; Sastry, C. V.; Maiya, B. G., to be published.

(38) Parker, C. A. *Photoluminescence of Solutions*; Elsevier Publishing Company: Amsterdam, 1968.

(39) Bhasikuttan, A. C.; Singh, A. K.; Palit, D. K.; Sapre, A. V.; Mittal, J. P. *J. Phys. Chem. A* **1998**, *102*, 3470.

(40) Berlman, I. B. *Handbook of fluorescence spectra of aromatic molecules*; Academic Press: New York, 1971.

(41) Pavia, D. L.; Lampman, G. M.; Kriz, G. S. *Introduction to Spectroscopy*; G. S. Saunders College Publishing: USA, 1979; p 292.

(42) Birks, J. B. *Photophysics of Aromatic Molecules*; Wiley-Interscience: London, 1969.

(43) *Conformational Analysis of Molecules in Excited state*; Waluk, J., Ed.; Wiley: New York, 2000.

(44) Schmidt, S. C.; Baldridge, K. K.; Boatz, J. A.; Elbert, S. T.; Gordon, M. S.; Jensen, J. H.; Koseki, S.; Matsunaga, N.; Nguyen, K. A.; Su, S. J.; Windus, T. L.; Dupiis, M.; Montogomery, J. A. *J. Comput. Chem*. **1993**, *14* 1347.

(45) Yip, W. T.; Levy, D. H.; Kobetic, R.; Piotrowiak, P. *J. Phys. Chem. A* **1999**, *103*, 10.

(46) Goldschmidt, C. R.; Ottolenghi, M. *Chem. Phys. Lett*. **1970**, *4*, 570.

(47) (a) Varnavski, O.; Samuel, I. D. W.; Pälsson, L.-O.; Beavington, R.; Burn, P. L.; Goodson, T. III. *J. Chem. Phys*. **2002**, *116*, 889. (b) Wang, Y.; Ramasinghe, M. I.; Goodson, T. III. *J. Am. Chem. Soc.* **2003**, *125*, 9562. (c) Ramasinghe, M. I.; Varnavski, O. P.; Pawlas, J.; Hauck, S. I.; Louie, J.; Hartwig, J. F.; Goodson, T. III. *J. Am. Chem. Soc.* **2002**, *124*, 6520.

(48) Kramers, H. A. *Physica* **1940**, *1*, 284.

(49) Fleming, G. R. In *Chemical Application of Ultrafast Spectroscopy*; Oxford University Press: New York, 1986; p 186.

(50) Waldeck, D. H. *Chem. Rev*. **1991**, *91*, 415.

(51) (a) Förster, T. *Ann. Phys.* **1948**, *2*, 55. (b) Förster, T. *Z. Naturforsch. A: Phys. Sci.* **1949**, *4*, 321.

(52) Van der Meer, B. W.; Coker, G. III; Simon Chen, S. Y. *Resonance Energy Transfer: Theory and Data;* VCH Verlog, Weinheim, Germany, 1944.

(53) Dexter, D. L. *J. Chem. Phys.* **1953**, *21*, 836.

(54) Monberg, E. M.; Kopelman, R. *Chem. Phys. Lett.* **1978**, *58*, 492.

(55) Klafter, J.; Jortner, J. *J. Chem. Phys.* **1981**, *75*, 2047.

(56) (a) Zhang, Y.; Sluch, M. I.; Somoza, M. M.; Berg, M. A. *J. Chem. Phys.* **2001**, *115*, 4212, (b). Jas, G. S.; Wang, Y.; Pauls, S. W.; Johnson, C. K.; Kuczera, K. *J. Chem. Phys.* **1997**, *107*, 8800.